PROCEEDINGS OF SCIENCE

New determination of the production cross section for γ rays in the Galaxy

Luca Orusa,[a,b,*] **Mattia Di Mauro,**[b] **Fiorenza Donato**[a,b] **and Michael Korsmeier**[c]

[a] *Department of Physics, University of Torino, via P. Giuria, 1, 10125 Torino, Italy*

[b] *Istituto Nazionale di Fisica Nucleare, via P. Giuria, 1, 10125 Torino, Italy*

[c] *The Oskar Klein Centre for Cosmoparticle Physics, Department of Physics, Stockholm University, Alba Nova, 10691 Stockholm, Sweden*

E-mail: luca.orusa@edu.unito.it

The flux of γ rays is measured with unprecedented accuracy by the *Fermi* Large Area Telescope from 100 MeV to almost 1 TeV. In the future, the Cherenkov Telescope Array will have the capability to measure photons up to 100 TeV. To accurately interpret this data, precise predictions of the production processes, specifically the cross section for the production of photons from the interaction of cosmic-ray protons and helium with atoms of the ISM, are necessary. In this study, we determine new analytical functions describing the Lorentz-invariant cross section for γ-ray production in hadronic collisions. We utilize the limited total cross section data for π^0 production channels and supplement this information by drawing on our previous analyses of charged pion production to infer missing details. In this context, we highlight the need for new data on π^0 production. Our predictions include the cross sections for all production channels that contribute down to the 0.5% level of the final cross section, namely η, K^+, K^-, K^0_S, and K^0_L mesons as well as Λ, Σ, and Ξ baryons. We determine the total differential cross section $d\sigma(p + p \rightarrow \gamma + X)/dE_\gamma$ from 10 MeV to 100 TeV with an uncertainty of 10% below 10 GeV of γ-ray energies, increasing to 20% at the TeV energies. We provide numerical tables and a script for the community to access our energy-differential cross sections, which are provided for incident proton (nuclei) energies from 0.1 to 10^7 GeV (GeV/n). This work is based on [1].

38th International Cosmic Ray Conference (ICRC2023)
26 July - 3 August, 2023
Nagoya, Japan

ICRC2023
38th International Cosmic Ray Conference
The Astroparticle Physics Conference

*Speaker

PoS(ICRC2023)264

1. Introduction

This work is based on [1], under the copyright licence number RNP/23/JUL/068240. Gamma rays (γ rays) represent the most energetic photons produced in the Universe. The Large Area Telescope (LAT) on board NASA's Fermi Gamma-ray Space Telescope (*Fermi*) [2] has revolutionized the field of γ-ray astronomy providing data with unprecedented precision. Ground-based experiments take advantage of their larger collective area and extend the energy range up to PeV scales [3]. Most of the γ rays detected by *Fermi*-LAT are produced by the Galactic insterstellar emission, which is generated by the interaction of charged cosmic rays (CRs, mostly proton and helium) with the atoms of the interstellar medium (ISM) or the low-energy photons of the interstellar radiation fields. The dominant processes are the hadronic interactions of CR nuclei with the gas of the Galactic disk [4]. The rate of interactions depends on the CR fluxes, the density of the ISM, and the inelastic production cross section $\sigma(p + p \rightarrow \gamma + X)$ (and similarly for a nuclear components in CRs and in the ISM). Improving the modeling of the γ-ray sky is a central topic in current research. In any case, a key ingredient to properly predict the hadronic γ-ray diffuse emission is the inclusive γ-ray production cross section $\sigma(p+p \rightarrow \gamma+X)$. Any uncertainty in these cross sections comparable or greater than the $Fermi$-LAT statistical errors undermine the study of the Galactic interstellar emission of the observed γ-ray sky. Since data are very limited for these cross sections, the standard approach is to determine them employing Monte Carlo event generators [5, 6]. There can be significant deviations between Monte Carlo generators for the production cross sections of γ rays (even larger than 30%). This demonstrates the necessity of improving our predictions for these cross sections. We present in this work a new and more precise model relying mostly on an analytic prescription. This strategy closely follows the one from [7] (hereafter ODDK22), where we derived cross sections for the secondary production of CR electrons and positrons.

2. From cross sections to the γ-ray emissivity

The hadronic component is a very important – often the dominant – contribution of the γ-ray flux. In the computation of the flux detected at Earth enters the emissivity ϵ at each location in the Galaxy $\vec{x}$, which is the convolution of the CR flux ϕ_i and the ISM density $n_{\rm ISM,j}$ with the energy-differential cross section for γ-ray production $d\sigma_{ij}/dE_\gamma$ for the reaction $i + j \rightarrow \gamma + X$:

$$\epsilon^{ij}(\vec{x}, E_\gamma) = n_{{\rm ISM},j}(\vec{x}) \int dT_i \, \phi_i(\vec{x}, T_i) \frac{d\sigma_{ij}}{dE_\gamma}(T_i, E_\gamma) \, . \tag{1}$$

We note that, in general, the emissivity depends on the position in the Galaxy. The vast majority of γ-ray photons are not directly produced in the proton-proton (or nuclei) collisions but rather by the decay of intermediate mesons and hadrons. The dominant channel is the production of neutral pions (π^0), and their subsequent decay into two photons. This channel is discussed in detail in Sec. 3, while we address the contributions from all other channels in Sec. 4. The γ-ray production cross section is derived from the π^0 production cross section convoluting this latter with the probability density function of the π^0 decaying into two photon. The fully differential production cross section is defined in the following Lorentz invariant form:

$$\sigma_{\rm inv}^{(ij)} = E_{\pi^0} \frac{d^3\sigma_{ij}}{dp^3_{\pi^0}} \, . \tag{2}$$

Here E_{π^0} is the total π^0 energy and p_{π^0} its momentum. The fully differential cross section is a function of three kinematic variables, for example, the center of mass energy $\sqrt{s}$, the transverse momentum of the pion p_T, and the radial scaling $x_R = E^*_{\pi^0}/E^{\max *}_{\pi^0}$, that is the ratio between the pion energy divided by the maximal pion energy in the center of mass frame(CM) labeled by a $*$. The energy-differential cross section is obtained by first transforming the kinetic variables from CM into the fix-target (LAB) frame, and then by integrating over the solid angle Ω.

3. γ rays from $p + p \rightarrow \pi^0 + X$ collisions

Given the relevance of the π^0 channel for the γ-ray production, it would be important to have precise data on a wide coverage of the kinematic phase space for the reaction $p + p \rightarrow \pi^0 + X$. Unfortunately, the available data are either not given for the double differential cross sections or affected by large systematics or do not cover the kinematic region relevant for Astroparticle physics. Instead, for the process $p + p \rightarrow \pi^{\pm} + X$ data for $\sigma_{\rm inv}$ has been collected by various experiments and large portions of the kinetic parameter space, as for example by NA49 [8]. Therefore, we decide to model $\sigma_{\rm inv}$ for the production of π^0 using the results of $\pi^{\pm}$ cross sections that we derived in ODDK22. We assume that $\sigma_{\rm inv}$ depends on kinematic variables by a relation between the shapes of the production cross sections of π^+ and π^- as derived in ODDK22, to which we refer for more details. Thus, for $p + p$ scattering we define $\sigma_{\rm inv}$ as:

$$\begin{aligned} \sigma_{\rm inv} &= \sigma_0(s)\, c_{20} \Big[G_{\pi^+}(s, p_T, x_R) \\ &\qquad + G_{\pi^-}(s, p_T, x_R) \Big] A(s), \end{aligned} \tag{3}$$

where $\sigma_0(s)$ is the total inelastic $p + p$ cross section, the functions G_{π^+} (G_{π^-}) represent the kinematic shapes of the invariant π^+ (π^-) cross section, and c_{20} is an overall factor that adjusts the total normalization of the cross section. The functions $G_{\pi^{\pm}}(s, p_T, x_R)$ are taken from ODDK22. The parameters c_1 to c_{19} in the definitions of $G_{\pi^{\pm}}$ are fixed to the values stated in ODDK22 (Tab. 2). Finally, the factor $A(s)$ allows adjusting the cross section to the measured π^0 multiplicities at different incident energies:

$$\begin{aligned} A(s) &= \left(1 + \left(\sqrt{s/c_{21}}\right)^{c_{22}-c_{23}}\right) \left(1 + \left(\sqrt{s/c_{24}}\right)^{c_{23}-c_{25}}\right) \\ &\quad \left(1 + \left(\sqrt{s/c_{26}}\right)^{c_{25}-c_{27}}\right) \left(\sqrt{s}\right)^{c_{27}} \Big/ A(\sqrt{s_0}), \end{aligned} \tag{4}$$

where $\sqrt{s_0}$ is fixed to 17.27 GeV, while the parameters from c_{20} to c_{27} are derived in this work. We focus on the scaling of the cross section at different $\sqrt{s}$. Our parametrization introduces the dependence on $\sqrt{s}$ through the function $A(s)$ that acts as an overall renormalization and we proceed with the determination of the parameters from c_{20} to c_{27}. To obtain a complete dependence from $\sqrt{s}$ we use the collection of total π^0 cross section measurements provided in Ref. [9] (in the following also called Dermer86). At larger $\sqrt{s}$ we fit the $x_F dn/dx_F$ data provided by LHCf [10] in the forward-rapidity region integrated for $p_T < 0.4$ at $\sqrt{s} = 2.76$ and 7 TeV, where $x_F = 2p_z/\sqrt{s}$ is the Feynman-x variable. In particular we consider only the data provided for $x_F < 0.7$, since the x_F shape of our $\sigma_{\rm inv}$ model determined in ODDK22 is tuned on [8] data, which cover $x_F < 0.7$ in

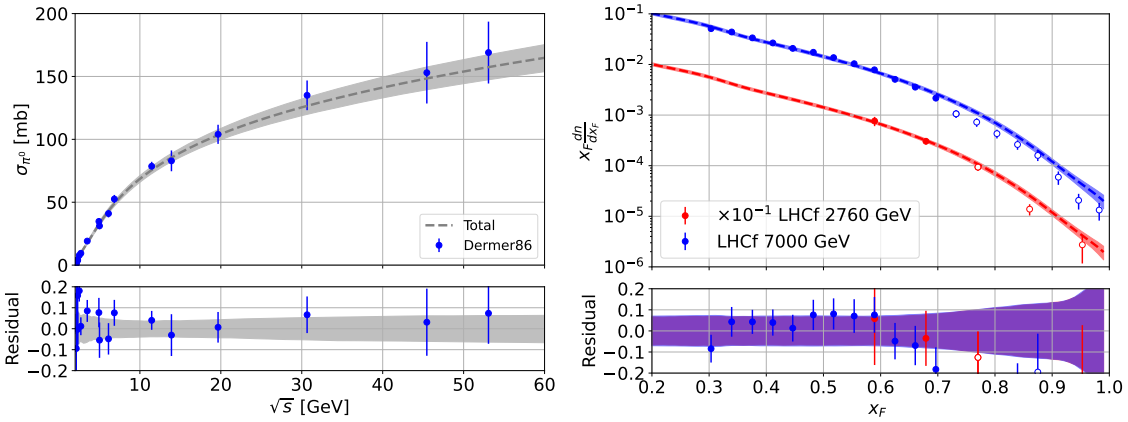

Figure 1: Total cross section (left panel) and $x_F dn/dx_F$ (right panel) of π^0 production in $p + p$ collisions measured at different $\sqrt{s}$. The solid lines represent the best-fit parametrization and the shaded bands show the uncertainty of our fit at the 1σ level. The bottom panels shows the residuals defined as (data-model)/model.

the low p_T region. We have verified a posteriori that the kinematic space of $x_F > 0.7$ contributes less than 2% of the final emissivity described by 1. The highest $\sqrt{s}$ of LHCf is 7 TeV, namely $T_p = 2.61 \times 10^7$ GeV in the LAB frame for a fixed target collision. Beyond this incident proton energy our parametrization must be considered as an extrapolation. We perform a χ^2 fit and use the MULTINEST [11] package to scan over the parameter space. Overall, our parametrization provides a good fit to the data sets at different $\sqrt{s}$. The χ^2 per number of degrees of freedom (d.o.f.) of the best fit converges to 26/24. The parameters from c_{20} to c_{27} are all well constrained by the fit and their values are reported in Tab. I of ODDK22. The results are displayed in Fig. 1. In the left panel, we report the fit to the low-energy data on the total cross section, while the right panel reports the fit to LHCf data. Within our parametrization, the π^0 total cross section is determined with a precision between 5% and 10% below $\sqrt{s}$ of 60 GeV (left panel). At LHCf energies the uncertainty varies between 5% and 10% below 0.7 with x_F, and increase to more than 10% for higher x_F values (right panel). There is a reasonable agreement between our predictions and the data also in the x_F range not considered in the fit.

The differential cross section for the production of γ-rays from $p + p \rightarrow \pi^0 + X$ scattering $d\sigma/dE_\gamma$ is obtained from $\sigma_{\rm inv}$. There are mainly three contributions to the uncertainty band: from the MULTINEST scan we obtained the best-fit value and the covariance matrix with correlated uncertainties of the parameters c_{20} to c_{27} and we numerically propagate this uncertainty by sampling the cross section parametrization for 500 realizations using the covariance matrix and assuming Gaussian statistics; the statistical uncertainties related to G_{π^+} and G_{π^-} functions; we also consider a systematic uncertainty for the kinematic shape, evaluating the difference of the cross section by assuming either a pure π^+ or a pure π^- kinetic shape (in Eq. (3) we replace $G_{\pi^+} + G_{\pi^+}$ by $2G_{\pi^+}$ or $2G_{\pi^-}$, respectively). Then, we derived the energy differential cross section from these two cases, compared the two results and use the maximal deviation as a function of energy as an additional contribution to the total uncertainty, which is obtained by adding all contributions in quadrature. Uncertainties on the differential cross section result to be between 6% and 20% for most of the energy range, except for E_γ close to T_p, where both statistical and systematic errors increase.

For most combinations of E_γ and T_p the statistical uncertainty dominates, while the systematic uncertainty due to the kinematic shape is at most at the same level as the statistical error. Only for a region of E_γ close to T_p, which is suppressed in the total emissivity, the systematic uncertainty dominates.

4. Contribution from other production channels and from nuclei

In this section we present our model for the photon production from further intermediate mesons and hyperons, and for scatterings involving nuclei heavier than hydrogen. Firstly photons are produced by the decay of K^+,K^-, K^0_S and Λ. We include their contribution by using the production cross sections derived in ODDK22. We calculate the spectra of photons assuming that π^0 are produced from a two or three body decay. The K^0_L meson is expected to give a contribution similar to the K^0_S meson. Due to the lack of experimental data we employ the Pythia event generator [12] to compare the p_T and x_F dependence of the final photon spectra from K^0_S and K^0_L, finding that their are very similar. The difference is approximately a normalization factor, with a production from the K^0_L of 1.16 times more than K^0_S. This is mainly due to the branching ratio of K^0_L into π^0 which is larger than for K^0_S. In the following we assume that the production cross section of γ rays from K^0_L is obtained from K^0_S by a rescaling of a factor 1.16.

$\bar{\Lambda}$, Σ and the Ξ give a subdominant contribution to the total photon yield. We thus have to add it into our calculations. We follow ODDK22 and estimate their contribution using the Pythia code [12], computing the multiplicities n_i as a function of E_p of each of these particles i. Then, we calculate the ratio n_i/n_Λ, both derived with Pythia. We use the ratio n_i/n_Λ to add these subdominant channels (S.C.) to the total yield of γ by rescaling the Λ cross sections into a γ-ray one. In this way we rely on the data-driven invariant cross section of Λ, which has a comparable mass to all these particles(the dependence of their cross section with the kinematic parameters is similar). Specifically, we use the following prescription: $d\sigma/dE_{\gamma \mathrm{S.C.}} = d\sigma/dE_{\gamma\Lambda} \times \sum_i \mathcal{F}^i(T_p)$ where $\mathcal{F}^i(T_p)$ represents the correction factor for each particle. For example, for Σ particles it can be written as: $\mathcal{F}^\Sigma(T_p) = n_\Sigma(T_p) \cdot {B_r}^{\pi^0}_\Sigma / n_\Lambda(T_p) \cdot {B_r}^{\pi^0}_\Lambda$ where ${B_r}^{\pi^0}_\Sigma$ is the branching ratio for the decay of the Σ hyperon into neutral pions.

Another relevant channel for the production of photons is the η meson, which decays into $\eta \rightarrow \gamma\gamma$ ($B_r = 39.41\%$) plus others channels involving π^0. Cross section data for the production of η mesons have been recently measured by several experiments. These data are typically collected at mid-rapidity and the double differential cross section data is not available. We include the photons from the direct η decay ($\eta \rightarrow \gamma\gamma$) by using the measured ratio between its multiplicity with respect to the π^0 one, as a function of p_T, fitting the available data.

As for the inclusion of scatterings including nuclei, in either the CRs or in the ISM, we closely follow the prescriptions derived in ODDK22 for $\pi^\pm$, given the lack of any dedicated data. Specifically, if a π^0 is produced in collisions between projectile and target nuclei with A_1 and A_2 mass numbers, the G functions in Eq. 3 are corrected as in Eqs. (25)–(27) by ODDK22. The parameters in Eq. (26) are taken from Tab. V from ODDK22, where column π^+ (π^-) corrects the function G_{π^+} (G_{π^-}). The $K^\pm$ channel is modified analogously by using the columns 3 and 4 in Tab. V from ODDK22. For all the other channels, we assume a correction function which is the average from the K^+ and K^- ones.

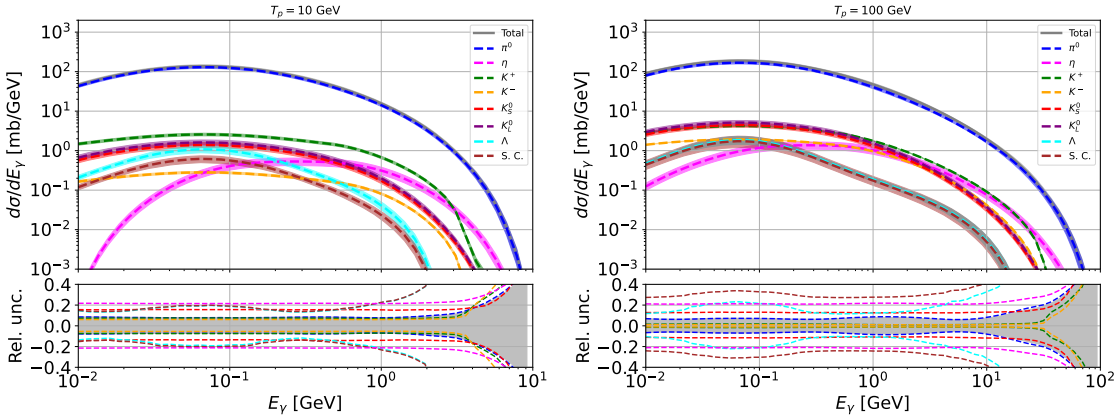

Figure 2: $d\sigma/dE_\gamma$ in $p + p$ collisions, derived from fits to the data as described in Secs. 3 and 4. We plot separate production of the different channels and their sum. Each plot is computed for incident proton energies T_p of 10 and 100 GeV. The curves are displayed along with their 1σ error band. At the bottom of each panel the 1σ uncertainty band is displayed around the best fit individually for each contribution.

5. Results on the γ ray production cross section and emissivity

We now can compute the total differential cross section $d\sigma/dE_\gamma$ shown in Fig. 2 for two representative incident proton energies summing all the contributions from π^0 and the subdominant channels. The contribution of $\pi^0 \rightarrow 2\gamma$ is dominant at all proton and photon energies. All the other channels contribute at most few percent of the total cross section. The gray curve and shaded band display the total $d\sigma/dE_\gamma$ and the 1σ uncertainty band, respectively. The final uncertainty spans from 6% to 20% at different T_p and E_γ, and is driven by the modeling of the π^0 cross section. For illustration, we compute the emissivity in Eq. 1 assuming a constant $n_{\rm ISM}$ and incident CR spectra independent of Galactic position. In Fig. 3 (left panel) we show $\epsilon(E_\gamma)$ as a function of E_γ for $p+p$, He+p, p+He, He+He and CNO+p scatterings, and their sum. We assume $n_{\rm H} = 0.9\,{\rm cm}^{-3}$ and $n_{\rm He} = 0.1\,{\rm cm}^{-3}$. Each prediction is plotted with the relevant uncertainty from the production cross section derived in this paper. The relative uncertainty to the total $\epsilon(E_\gamma)$ is reported in the bottom panel. As expected, the most relevant contribution comes for $p + p$ reactions. Nevertheless, the contributions from scatterings involving helium globally produce a comparable source spectrum. The uncertainty on $\epsilon(E_\gamma)$ due to hadronic production cross sections is about 10% for $E_\gamma \leq 10$ GeV, and increases to 20% at TeV energies. As a comparison, we report the results by [5] (Kamae,used in the *Fermi*-LAT official Galactic interstellar emission model [4]) and [6] (AAfrag) for the $p + p$ channel. We also show in Fig. 3 (right panel) a comparison between our cross section and the one derived by Kamae and AAfrag.

Our cross section is larger than Kamae at *Fermi*-LAT energies by a rough 5-10%. Also, the high energy trend of our cross section is slightly harder than Kamae and AAfrag. The emissivity shown in Fig. 3 (left panel) is comparable or slightly higher than the Kamae and AAfrag ones. Fig. 3 (right panel) shows how our model predicts similar or slightly higher values of the cross-section for those E_γ produced in the forward direction, that are the relevant ones for the emissivity in the plotted energy range. In the relevant energies for *Fermi*-LAT, the results obtained in this paper are however compatible with Kamae and AAfrag at 1σ of the estimated uncertainty bands.

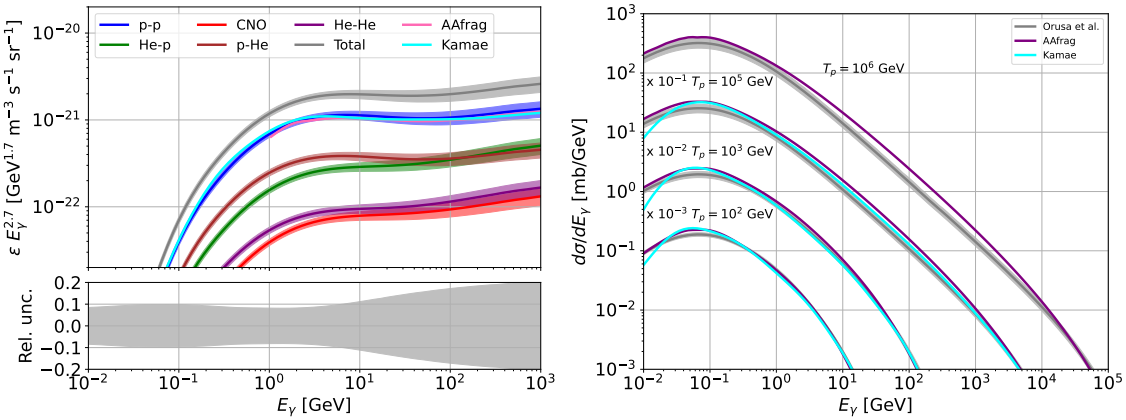

Figure 3: Left panel: γ-ray emissivity computed for $p + p$, He+p, p+He, He+He and CNO+p scatterings. The grey line is the sum of all contributions. Each prediction is plotted with the relevant uncertainty due to $d\sigma/dE_\gamma$ derived in this paper. In the bottom panel, the relative uncertainty to the total $\epsilon(E_\gamma)$ is reported. For comparison, we show the results by [5] (Kamae) and [6] (AAfrag) in the $p + p$ channel. Right panel: Comparison among our differential cross section and the one of Kamae and AAfrag, for four incident proton energy. The three lower curves have been rescaled by the factor indicated in the figure for the sake of visibility.

6. Discussion and conclusions

The diffuse Galactic emission is dominated by the decay of neutral pions, in turns produced by the inelastic scattering of nuclei CRs with the ISM. A precise modeling of the production cross section of γ rays of hadronic origin is crucial for the interpretation of data coming from the *Fermi*-LAT, for which the diffuse emission is an unavoidable foreground to any source or diffuse data analysis. In this paper, we propose a new evaluation for the production cross section of γ rays from $p + p$ collisions, employing the scarce existing data on the total cross sections, and relying on previous analysis of the cross section for $e^{\pm}$. The cross section for scattering of nuclei heavier than protons is also derived. Our results are supplied by a realistic and conservative estimation of the uncertainties affecting the differential cross section $d\sigma/dE_\gamma$. This cross section is estimated here with an error of 10% for $E_\gamma \leq 10$ GeV, increasing to 20% at 1 TeV. We also provide a comparison with the cross sections implemented in the official model for the *Fermi*-LAT diffuse emission from hadronic scatterings. It turns out that our cross section is higher than the one in [5] by an average 10%, depending on impinging protons and γ-ray energies. This result is relevant for the *Fermi*-LAT data analysis in the regions close to the Galactic plane, where hadronic scatterings with ISM nuclei are the main source of diffuse photons.

In order to improve the accuracy of the present result, new data from colliders are needed. Specifically, data is required on the Lorentz invariant cross section, and not only on the total cross section, for π^0 productions. The most important kinetic parameter space is $p_T \lesssim 1$ GeV, a large coverage in x_R and beam energies in the LAB frame covering from a few tens of GeV to at least a few TeV. It would be important to get the same measurements also on a He target.

We provide numerical tables for the energy-differential cross sections $d\sigma/dE_\gamma$ as a function of the E_γ and incident proton (nuclei) energies from 0.1 to 10^7 GeV (GeV/n), and a script to read them. The material is available at https://github.com/lucaorusa/gamma_cross_section.

References

[1] L. Orusa, M. D. Mauro, F. Donato, and M. Korsmeier, *New determination of the production cross section for γ rays in the galaxy*, *Physical Review D* **107** (apr, 2023).

[2] **Fermi-LAT** Collaboration, W. B. Atwood et al., *The Large Area Telescope on the Fermi Gamma-ray Space Telescope Mission*, *Astrophys. J.* **697** (2009) 1071–1102, [arXiv:0902.1089].

[3] **LHAASO** Collaboration, A. Addazi et al., *The Large High Altitude Air Shower Observatory (LHAASO) Science Book (2021 Edition)*, *Chin. Phys. C* **46** (2022) 035001–035007, [arXiv:1905.0277].

[4] **Fermi-LAT** Collaboration, F. Acero et al., *Development of the Model of Galactic Interstellar Emission for Standard Point-Source Analysis of Fermi Large Area Telescope Data*, *Astrophys. J. Suppl.* **223** (2016), no. 2 26, [arXiv:1602.0724].

[5] T. Kamae, N. Karlsson, T. Mizuno, T. Abe, and T. Koi, *Parameterization of Gamma, e+/- and Neutrino Spectra Produced by p-p Interaction in Astronomical Environment*, *Astrophys. J.* **647** (2006) 692–708, [astro-ph/0605581]. [Erratum: Astrophys.J. 662, 779 (2007)].

[6] S. Koldobskiy, M. Kachelrieß, A. Lskavyan, A. Neronov, S. Ostapchenko, and D. V. Semikoz, *Energy spectra of secondaries in proton-proton interactions*, *Phys. Rev. D* **104** (2021), no. 12 123027, [arXiv:2110.0049].

[7] L. Orusa, M. Di Mauro, F. Donato, and M. Korsmeier, *New determination of the production cross section for secondary positrons and electrons in the Galaxy*, *Phys. Rev. D* **105** (2022), no. 12 123021, [arXiv:2203.1314].

[8] **NA49** Collaboration, C. Alt et al., *Inclusive production of charged pions in p+p collisions at 158 gev/c beam momentum*, *Eur. Phys. J. C* **45** (Dec, 2005) 343–381.

[9] C. D. Dermer, *Binary collision rates of relativistic thermal plasmas. ii-spectra*, *The Astrophysical Journal* **307** (1986) 47–59.

[10] O. Adriani et al., *Measurements of longitudinal and transverse momentum distributions for neutral pions in the forward-rapidity region with the LHCf detector*, *Physical Review D* **94** (aug, 2016).

[11] F. Feroz, M. P. Hobson, and M. Bridges, *Multinest: an efficient and robust bayesian inference tool for cosmology and particle physics*, *Monthly Notices of the Royal Astronomical Society* **398** (Oct, 2009) 1601–1614.

[12] T. Sjöstrand, S. Ask, J. R. Christiansen, R. Corke, N. Desai, P. Ilten, S. Mrenna, S. Prestel, C. O. Rasmussen, and P. Z. Skands, *An introduction to PYTHIA 8.2*, *Comput. Phys. Commun.* **191** (2015) 159–177, [arXiv:1410.3012].

PoS(ICRC2023)264